Ceramics International 45 (2019) 13664–13670

Contents lists available at ScienceDirect

Ceramics International

journal homepage: www.elsevier.com/locate/ceramint

Vertically oriented graphene nano-sheets grown by plasma enhanced chemical vapor deposition technique at low temperature

Ozkan Bayram[a,*], Onder Simsek[b]

[a] Bayburt University, Engineering Faculty, Electrical and Electronics Engineering, TR-69100, Bayburt, Turkey
[b] Ataturk University, Graduate School of Natural and Applied Sciences, Department of Nanoscience and Nanoengineering, TR-25240, Erzurum, Turkey

ARTICLE INFO

Keywords:
Vertically-oriented graphene
Raman
PECVD

ABSTRACT

In this study, it was aimed to obtain vertically-oriented graphene nano-sheets (VGNs) on copper foils using CH_4 gas as the precursor material by means of plasma enhanced chemical vapor deposition (PECVD) technique. VGNs were obtained at 50 W, 75 W and 100 W Radio Frequency (RF) powers by this technique and the effect of RF power on the morphological structure of graphene layers was investigated. VGNs were also analyzed by Raman spectroscopy, scanning electron microscopy (SEM) and water contact angle (WCA) measurements. The SEM images showed that the VGNs became more tightly packed with the increase of RF power and thus these coating parameters had a significant effect on the morphological structure. WCA analyzes for VGNs were also performed and it was found that VGNs obtained at 100 W RF power had higher contact angle value than the other RF powers. These VGNs, which have both large surface area and optically transparent, are thought to be materials that have the potential to be used in supercapacitors and solar cells.

1. Introduction

The graphene structures, discovered by Novoselov and his colleagues [1] for the first time by the mechanical exfoliation of graphite, have greatly received interest by the scientists since then. Two-dimensional (2D) graphene, which has superior thermal conductivity [2], high carrier mobility [3], optical [4] and mechanical [5] properties, has the potential to use in important areas such as sensors [6,7], solar cells [8,9], energy storage [10] and electronic devices [11]. Recently, 2D graphene, which has optically transparent and excellent mechanical strength, has further increased its current interest [12,13]. Moreover, due to its unique electron-band structure and electron transport properties, the new generation of high-performance modulators, which can operate in the infrared (IR) spectral region, are perceived as alternative materials for sources and detectors [14,15].

2D graphene, which can be obtained as single layer or multiple layers, is considered an important material for many applications due to the number of layers that can be adjusted. Mechanical exfoliation and chemical vapor deposition (CVD) techniques are the most commonly used techniques for obtaining graphene films of chemically highest quality and number of different layers. In particular, it is considered by many researchers that the CVD method is very low-cost method for obtaining monolayer graphene. Nickel or copper foils are generally used as catalyst substrates in this process. Flores et al. [16], performed the transfer of the graphene nanostructures obtained on copper foil using CVD technique to another insulated substrate in order to determine the electrical and optical properties of the graphene nanostructures. The mechanical stress on the film surfaces and foreign atoms that occur during the transfer process of graphene to these substrates are negative factors affecting the thin film quality. In order to minimize these negative effects, a great deal of research has been carried out by some researchers on both production techniques and transfer processes. In a study conducted by Zhang et al. [17], they were developed a new alternative to traditional transfer method. Here, it is aimed to minimize the impurities caused by foreign atoms occurring during the transfer process. On the other hand, new approaches are introduced in terms of production techniques. Graphene nanostructures, which can be produced as 2D, are also produced as vertically oriented (3D) depending on the used production technique recently. Vertically oriented graphene nanostructures have the potential to be used in fuel cells [18], field emitters, lithium ion batteries [19,20] and supercapacitors [21]etc. due to its large surface areas and optically transparent [22–25]. In a study by He et al. [26], they reported that there was a numerical model available for the growth of the monolayer graphene, but on the other hand there was no exact model for multilayered graphene and vertically oriented growth.

Micro-Raman spectroscopy is widely used to study carbon-based materials such as carbon nanotubes and graphene [27–33]. By using

* Corresponding author.
E-mail addresses: obayram@bayburt.edu.tr, ozkanbayram5555@hotmail.com (O. Bayram).

https://doi.org/10.1016/j.ceramint.2019.04.034
Received 16 February 2019; Received in revised form 21 March 2019; Accepted 3 April 2019
Available online 07 April 2019

this spectroscopy technique, it can be determined that the graphene structures are either single layer or multilayer and that the growth is homogeneous or heterogeneous. Therefore, this spectroscopy technique is an essential technique for the analysis of materials such as carbon-based graphene. In this article, by using copper foils as metal catalyst, it is aimed to obtain 3D graphene structures using PECVD technique at relatively low temperatures. These VGNs were transferred to insulating substrates by simple transfer approach developed by Zhang et al. In addition, it was investigated by Raman spectroscopy to determine the homogeneity of these VGNs and the presence of graphene structure. SEM analysis was also performed to determine the effect of RF power on the surface morphology of thin films.

2. Materials and method

Monolayer or multi-layer graphene were produced on copper foils at growth temperature of 750 ^{0}C and at various RF powers such as 50 W, 75 W and 100 W by using PECVD technique. The PECVD system produced by Nanovak (Turkey) is that allows graphene to be obtained at relatively low temperatures. In this study, 25 μm thickness copper foils used as substrate material were purchased commercially from *Alfa Aesar (99.8%, NO.13382)*. The graphene nanostructures obtained on copper foils were then transferred to glass substrates and these transferred graphene nanostructures were characterized. Graphene transfer process can be explained as follows. Here, a polymer-free biphasic (liquid/liquid) approach developed by Zhang et al. [17] was used to transfer single or multiple layered graphene onto various substrates. In this approach, the ether layer and the organic layer (hexane), which is an inert, non-polar and low viscosity, were used to etching the Cu layer. Ammonium peroxodisulfate $(NH4)_2S_2O_8$), commercially available from Sigma Aldrich was used as the ether layer. This solution, which was set to 0.1 M, was first filled into an empty beaker and the copper/graphene material was placed in this solution, provided that the graphene-covered surface remained on the upper surface. Here, hexane was used instead of the polymer layer used in other conventional transfer methods. Another important reason for the use of hexane is to ensure that the remaining graphene layer after the etching of Cu substrate is not exposed to etchant layer. Deionized (DI) water was used as the rinsing process. The steps of etching the copper foil are detailed in Fig. 1 [17]. Furthermore, the demonstration of this event was shown in Fig. 2 [17].

It may be more useful to describe the graphene production process as three steps. The copper foils were first cut to 2 cm × 2 cm and then each foil was subjected to wet cleaning. The wet cleaning process was carried out using various alcohols, also known as standard cleaning process. Each foil was purged with acetone, isopropanol and DI water in the standard cleaning process, respectively. Each procedure was performed for 30 s. The DI water-washed foils were dried in nitrogen gas atmosphere, and then stored at low pressure. Secondly, graphene nanosheets were aimed to be obtained on copper foils using PECVD technique. These graphene nanostructures were produced using the PECVD system shown in Fig. 3. [67].

CH_4 gas was used as the carbon source in the production of VGNs. H_2 gas was used as the CH_4 diluent, and Ar gas, which is high energy and inert, was used to obtain graphene at relatively lower temperatures. Thin films were obtained by using 50 W, 75 W and 100 W RF powers values and 30 min coating time. Before each coating process, the copper foils placed in the bottom layer of the PECVD system were first annealed at 1000 °C. The annealing was carried out for 15 min using 20 sccm H_2 gas. After the annealing process was completed, the temperature of the vacuum chamber was reduced to 750 °C. Coatings were performed at this temperature value using 7 sccm CH_4, 20 sccm H_2 and 10 sccm Ar gas, respectively. In addition, coating time was 30 min and above-mentioned RF powers were used to obtain graphene nanostructures. After the coating process, the CH_4 gas flow was cut off and cooled down to room temperature using H_2 and Ar gas. In the cooling process, the gas flow rates of both gases were as in the growth process. After the coating process was completed, the transfer of the graphene produced on copper foil to the insulating substrates was carried out. Graphene transfer was done by etching process of copper foils. And then, the graphene structures were transferred onto the glass substrates. The analysis of the transferred VGNs were performed using Raman, WCA and SEM, respectively. It is also aimed to confirm the number of graphene layers by Raman spectroscopy. Surface morphologies of thin films were also investigated by SEM analysis. Wrinkles and defects on VGNs surfaces were investigated by this spectroscopy technique.

3. Results and discussions

3.1. Raman analyses of VGNs

The results of Raman spectroscopy of VGN obtained by plasma enhanced chemical vapor deposition technique are presented in Fig. 4, and this Figure was interpreted in detail. Raman spectroscopy is basic

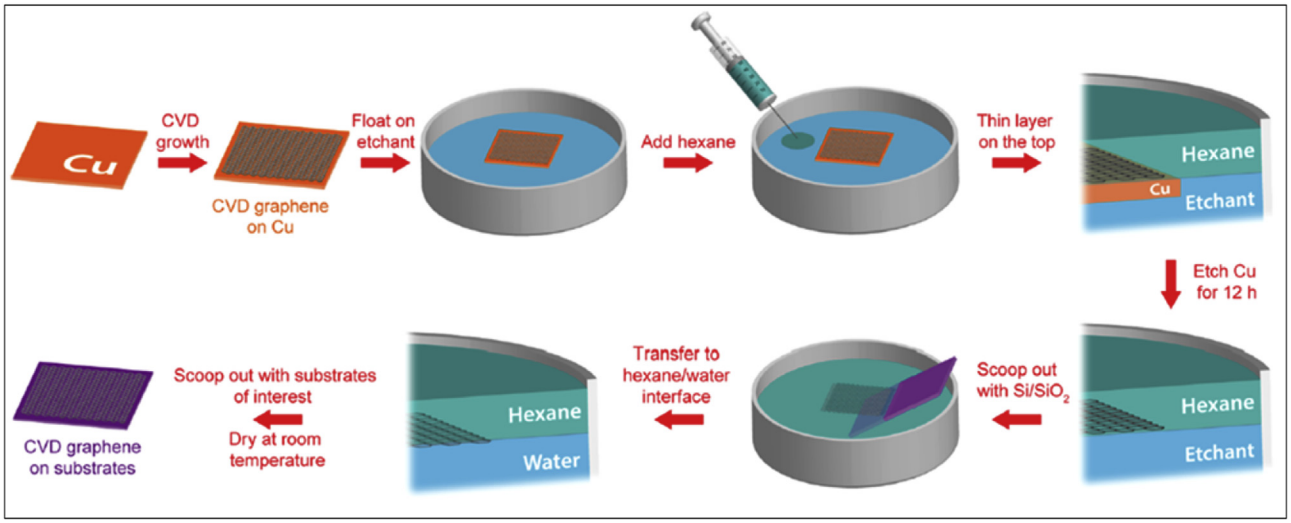

Fig. 1. The etching of the copper foil is carried out sequentially as described above. For the transfer of the VGN on the glass substrate, the amount of solution required for the etching of copper having a size of 2cmx2cm was determined mathematically. Because the addition of too much or too little solution for etching may not be sufficient for etching the desired level of copper. Please refer to the Supporting Information S1.

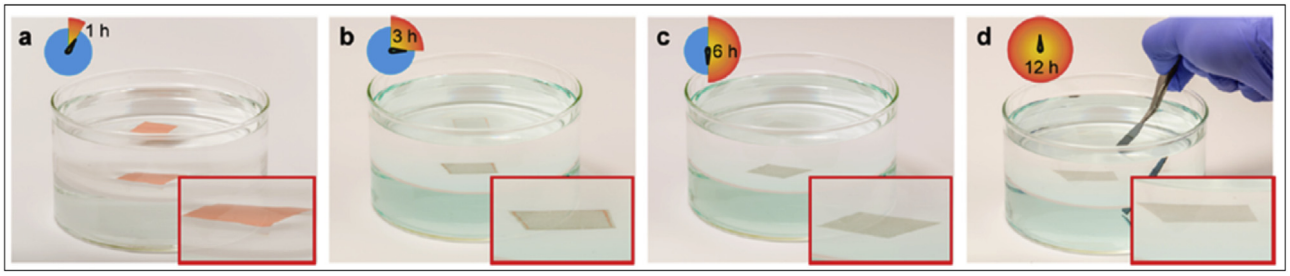

Fig. 2. The etching process was carried out according to the steps indicated in the relevant reference and these steps were completed about 12 hours (Supporting Information S2.).

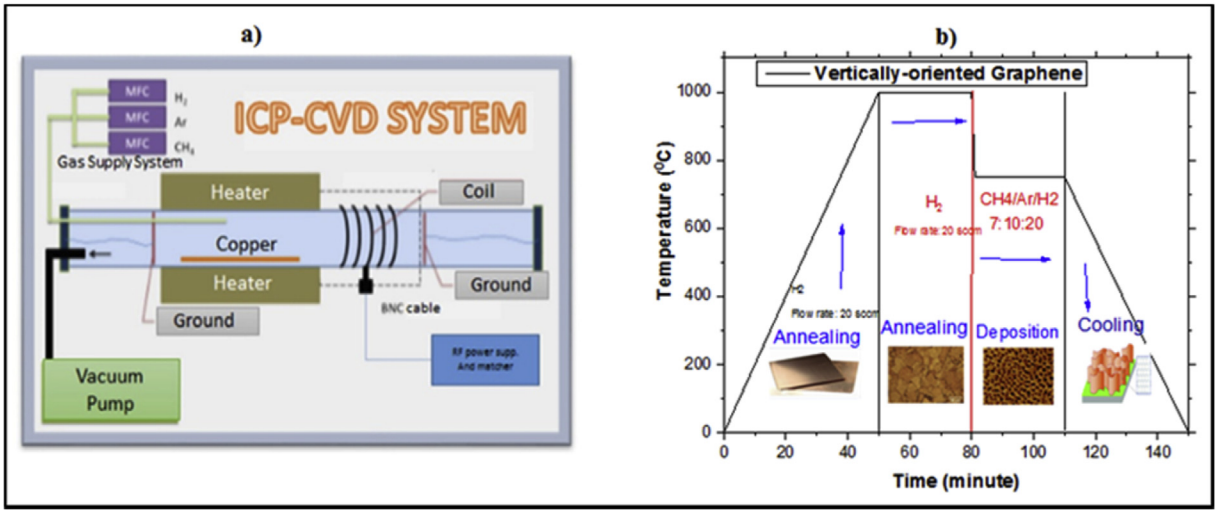

Fig. 3. (a) On the left, there is a schematic representation of the PECVD system used in this study. The system was established by the Nanovak company. It consists roughly of the furnace, vacuum chamber, vacuum pump, gas flow unit and RF power supply. The whole system can be controlled simply. (b) The steps of obtaining VGNs are described gradually. In this presentation, temperature, gas flow rates and deposition time are presented in detail.

method commonly used to determine the number of graphene layer. Carbon based materials such as graphene are represented by five major peaks in these spectra obtained from this analysis [27,31,34–42]. Each peak represents important information for the structure. These peaks are D, G, D', 2D and D + G peaks, respectively, according to the increasing wavenumber. The D-peak, which corresponds to the phonon mode and is attributed to the presence of defects in the structure and the intensity of the defects, is one of the most important among these peaks. Another is G peak, which is the E_{2g} mode and is attributed to the stretching of the *C*-C bond. A strong peak at approximately 2680 cm^{-1} for graphene nanostructures, represents the 2D peak, an important peak for sp2 carbon materials along with the G peak. This peak is also decisive for determining the number of layers of graphene. The 2D peaks for multi-layered graphene are quite weak and broad, whereas in the monolayer graphene, this peak is rather sharp and dense. The desired monolayer graphene structure associated with the presence of a substantially weak D peak. However, the presence of 2D and G peaks and their severity relative to each other are important to determine the presence of monolayer graphene. The presence of D-peaks associated with defects for graphene nanostructures grown with the PECVD technique was noted in previous studies [43–45]. As the cause of these defects can be shown as the presence of plasma. During the plasma enhanced growth process, radical molecules are localized due to dot-defects. In the film growth process, the presence of the excess reactive hydrogen atom present in the plasma triggers *C*-H strains. This leads to *C*-H stretching on the graphene nanosheets [46,47]. This is evidence of the D' peak observed at approximately 2950 cm^{-1} in all the structures obtained within the scope of our study. The 2D peaks for multi-layered graphene are quite weak and broad, whereas in the monolayer graphene, this peak is rather narrow and sharp. For the desired monolayer graphene, the D-peak is weak or even unrepresentative, indicating a perfect structure. However, the presence of 2D and G peaks and their severity relative to each other are important to determine the presence of monolayer graphene [31,48,49]. Raman spectroscopy contains an important information about the structural properties of graphene, the intensity and width of these peaks and the wavenumbers in which the aforementioned characteristic bands occur. The presence, intensity and proportions of these bands were investigated in order to characterize the graphene structural properties obtained at various RF powers at a relatively low temperature of 750 ° C. As can be seen from Fig. 4, for all films, the base peaks were determined at 1345 cm^{-1}, 1590 cm^{-1}, 2688 cm^{-1} and 3248 cm^{-1}. Here, the sharp peak at 1345 cm^{-1} is attributed to the D-band and the bands at 1588 and 2688 cm^{-1} are G and 2D bands, respectively, where the intensity of these two bands has changed significantly depending on the increased RF power.

No significant change was observed in these characteristic peaks of VGNs due to their position in the wave numbers. However, significant change was observed in the 2D peak of the VGN obtained using 75 W RF power. The detailed view of the 2D peaks of VGNs is given in Supporting Information Fig. S4. In Raman spectroscopy, the number of graphene layers is determined by the position, intensity and proportions of the these characteristic peaks. The intensity ratio between the 2D band and the G band indicates the number of graphene layers and is determined by the I_{2D}/I_G ratio [50]. If this ratio is greater than 2 [51], the single layer is classified as two-layer if it is between 1 and 2 [52] it is three or more layers if less than 1 [53].

I_{2D}/I_G ratios of VGN obtained at 50 W, 75 W and 100 W RF power were determined as 0.52, 0.71 and 0.78, respectively. These results are

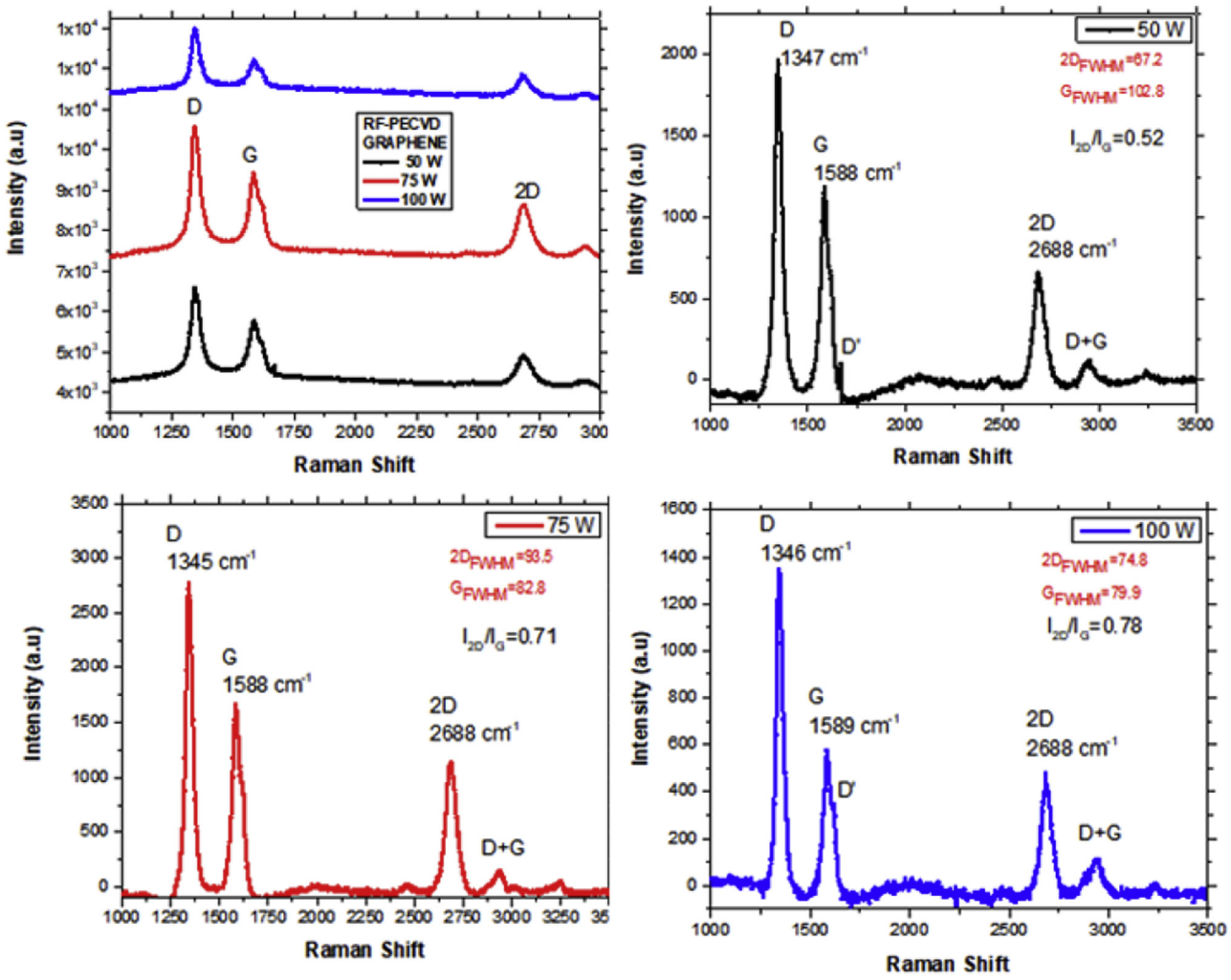

Fig. 4. The graph includes the Raman spectra for all VGNs at the top of the left. In this graph, D, G, D′ and 2D peaks and their proportions and their intensity are clearly indicated. However, other graphs show Raman analyzes for each VGNs. In these analyzes, the intensities of each peak and I_D/I_G and I_{2D}/I_G values are given, which are important for graphene. FHWM values are also presented in this graph (For the Raman spectra, the subtract baseline was performed) (Supporting Information S3).

interpreted that the graphene obtained by PECVD technique is three or multilayer and these results are in good agreement with the literature. Another analysis used to determine the number of graphene layers is the determination of the full width at half maxium (FWHM) values of the peaks. When the FWHM values of G and 2D peaks of all graphene films are compared, it is understood that it is compatible with the ratio of I_{2D}/I_G. As stated in the literature studies, the increase in the number of graphene layers leads to an increase in the FWHM value of the 2D peak, while the decreasing leads to a decrease in this FWHM value. According to the increasing RF power, FWHM values of 2D peak were determined as 67.2 cm^{-1}, 82.8 cm^{-1} and 74.8 cm^{-1}, respectively. Terasawa et al. [36] reported that, the FWHM value for single layer graphene was less than ~ 35 cm^{-1}, and that this value was greater than 65 cm^{-1} for three layer graphene. The results obtained from the FWHM values and I_{2D}/I_G ratio of VGNs indicate that the VGNs are three or more layered [54]. The I_{2D}/I_G ratio is typically ~2 for the monolayer graphene and for the two-layer graphene this ratio falls to 1.2 [16,17]. For the single layer graphene, the FWHM value of the 2D peak is ~35 cm^{-1} and for three - layer graphene this value is greater than 65 cm^{-1} [18,19]. The FWHM value for the 2D peak of the VGN obtained at 100 W RF power is greater than 65 cm^{-1} and this value was determined as 74.8 cm^{-1}. This value refers to the three-layer graphene structure. On the other hand, FWHM values of VGNs obtained for 50 W and 75 W were determined as 67.2 cm^{-1} and 82.8 cm^{-1}, respectively, and attributed to at least three-layer graphene structure. However, the value I_D/I_G also provides important information for graphene structures. In general, the higher I_D/I_G value and the increased FWHM values of the characteristic bands mean smaller crystalline particles and therefore smaller inter-error distance. I_D/I_G values were 1.64, 1.66 and 2.25, respectively, according to the increased RF power. Kurita et al. [55], reported that the crystallite size of VGN can be calculated from the value I_D/I_G, and these results were also extensively approved by many researchers. The crystallite size abovementioned is defined by the empirical equation of Cancado et al. [56], which is explained by the relationship between the in-plane sp2 crystallite size La, the laser source excitation energy E_l and I_D/I_G [57],

$$\frac{I_D}{I_G} = \frac{C_\lambda}{L_a}$$

where λ is the wavelength of light and C (λ) is a constant known as C (λ) = 2.4 Å [56]. The crystallite sizes calculated from the above equation for the ratios of 1.64, 1.66 and 2.25 of I_D/I_G were determined as 14.5, 14.4, 10.6 nm, respectively. In a study conducted by Terasawa et al. [36], these values were reported to be 14 and 26 nm, respectively, for VGN obtained at 900 ^{0}C and 500 ^{0}C using 300 W RF power. Literature studies indicate that the presence of increased RF power leads to high-density plasma and consequently the growth of graphitic

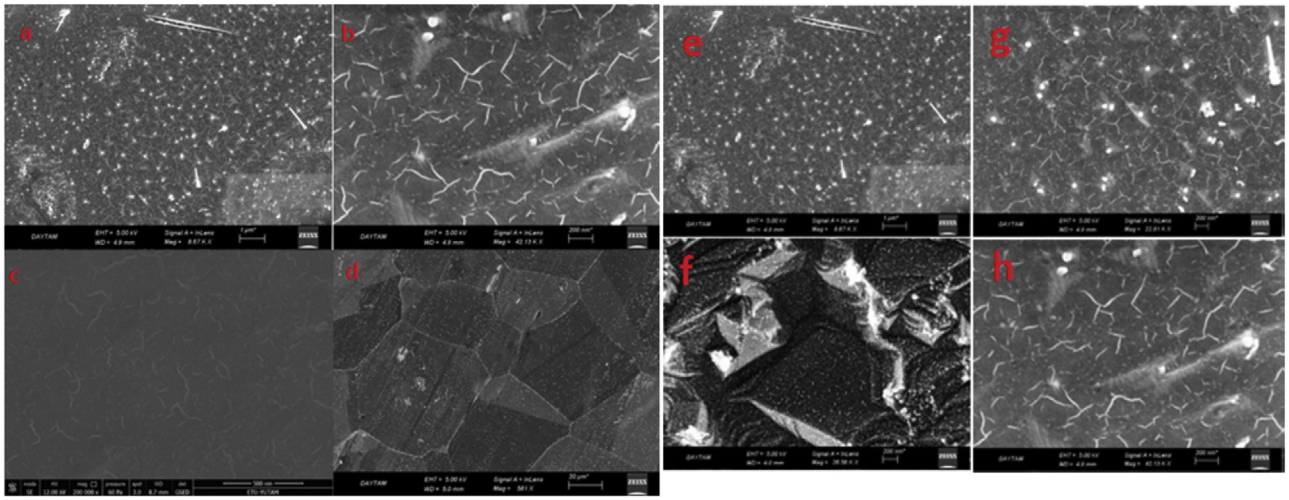

Fig. 5. These graphs are presented as the simplest proof that vertical-oriented graphene layers are obtained. VGNs were successfully obtained for 50 W, 75 W and 100 W RF Powers, respectively, and the graphs above were given at different magnifications. a-d belongs to the VGN obtained at 50 W RF power and relatively weak VGNs are seen compared to others. The rate of magnification from a to c is also increasing, so the change of VGNs morphologies from the graphics is also understood. d represents the grain boundaries of copper foil and growth within these grain boundaries. e-f and g-h are similarly representative of VGNs obtained using RF power of 75 W and 100 W, respectively.

structures. Here, it is not always possible to make a correct conclusion by comparing the values of I_D/I_G, taking into account the I_D peak representing the defect structures. The process of producing graphene using the PECVD technique is a highly complex process, so it is not correct to suggest that RF power is the only important parameter affecting the quality of the obtained product. In addition to the RF power, other important parameters such as H_2, CH_4 and Ar gas flow rates, temperature and coating time should be taken into consideration.

3.2. Surface morphologies of VGNs

Fig. 5 (a) - (h) represent SEM images of VGNs deposited at various RF powers, at a temperature of 750 ˚ C and a coating time of 30 min. It is understood that RF power significantly affects the morphology of the obtained VGNs. Fig. 5 (a) shows the growth rate of VGNs obtained for 50 W RF power, and it is understood that VGNs represent the structure, although not tightly packed, provided that the 3D graphene structure is homogeneous. Significant differences in the morphologies of VGNs obtained at relatively low temperatures are attributed to the RF power. The precursor gas (CH_4), which is responsible for the growth of VGNs, is activated by breaking down due to H_2 gas and Ar gas in the vacuum chamber. H_2 gas is used for dilution of CH_4 and Ar gas is used to aid in the decomposition of CH_4 by increasing collisions of Ar atoms due to RF power. The difference in the growth rates of VGNs at a temperature that can be considered to be relatively low temperature is attributed to the applied RF power.

Although Guo et al. [58], suggested that the VGNs can not be obtained at temperatures below 800 ˚C, the results of our study have not confirm this. Their study reports that homogeneous VGNs were obtained up to 800˚. That is, the kinetic energy of the carbon-containing radicals should remain stable by adjusting the growth parameters (temperature and CH_4/H_2 gas flow rates). The VGN mechanism is carried out by diluting the weakly bound carbon atoms with the appropriate H_2 concentration to form the graphitic structure [59]. In contrast, Sui et al. [60], showed that VGNs in the range of 750 ˚C and 700 ˚C were available by adjusting the coating parameter such as coating time and pressure. Also, Sui et al. showed that the coating time had a significant effect on the formation of VGNs and that Ar plasma pretreatment triggered VGN growth [60]. When pretreatmented using Ar plasma, the formation of VGNs is facilitated. Both the pretreatment with Ar plasma and the optimum value of the temperature are the most important parameters for the formation of VGNs. The fact that VGNs can be obtained directly on the insulating substrate at relatively low temperatures provides considerable benefit for the possible applications of these graphene structures. The greatest benefit here is that the defects that occur during the transfer of graphene to another substrate are eliminated. In our study, VGNs obtained with 75 W and 100 W RF power are in good agreement with the literature studies [61–63]. Obtaining VGN by PECVD technique can be explained as follows. During the first stage of growth on the substrate surface, the graphene layers grow in 2D orientation on the substrate. Due to the electric field in the plasma, the upper layers of the graphene are now subject to stress due to the force caused by this electric field, and curved structures begin to form on the surfaces. The graphene layers growing on the substrate tend to grow in 3D due to the sufficient tensile energy between this substrate and the graphene layer [60]. A representative image 3D oriented graphene nanosheets growth is shown in Fig. 6.

3.3. WCA measurements of VGNs

The wettability of the material used as the substrate can vary substantially with the coating process. Water contact angle (WCA) measurements (Fig. 7) showed that the applied RF power had a significant effect on the wettability measurements. For the VGN transferred to the glass substrate, the WCA values were measured at 86, 99 and 102˚, respectively, depending on the increased RF power, and this value was 26˚ for uncoated glass substrate. Further, the degree of hydrophobicity can be further increased or adjusted with the coating time. In a study conducted by Ci et al. [64], they reported that WCA values of VGNs grown at various coating times ranged from 80 to 128˚. In a study conducted by Ghosh et al. [65], they showed that the growth temperature significantly increased the WCA value of the surface. The reason for this increase is attributed to the VGN surface morphology, chemical bond structure, oxygen functionality, and crystallinity. The hydrophobic surface property, which can be adjusted depending on the number of VGN layers, shows that it can be used in many useful applications such as self-cleaning windows and water collection device. Jacob et al. [66], reported that using the *Melaleuca Alternifolia* essential oil as an initiator monomer, the graphene films produced by the PECVD technique exhibited a constant water contact angle of 135˚. They also claimed that this result was the highest reported contact angle value for graphene films produced with a bottom up method (PECVD) and having

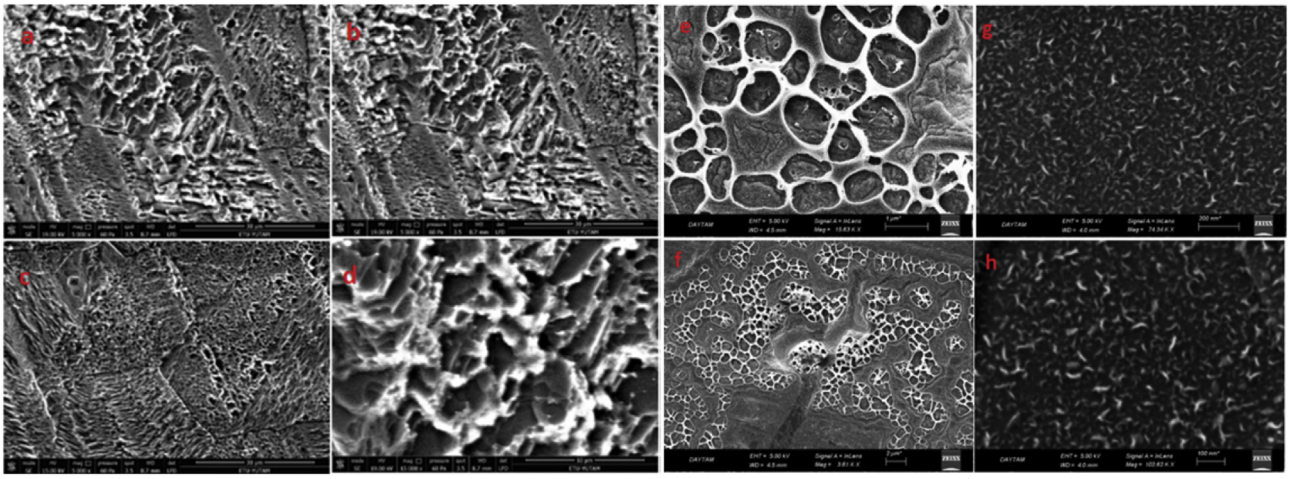

Fig. 6. For each of the three VGN, SEM patterns were obtained at various magnifications. Vertical-oriented growth is clearly seen from these images. According to increasing RF power, significant changes in the shape and density of VGNs were detected. It is evident that a-d images, VGN obtained for 50 W RF power are homogeneous morphology. e-f is the morphological structure of the VGN obtained at a power of 75 W RF, and there is clearly a growth in hexagonal growth. The g-h images represent the VGN obtained for 100 W RF power, and it is seen that the vertical orientation growth in both e and f is homogeneous and has the same morphology.

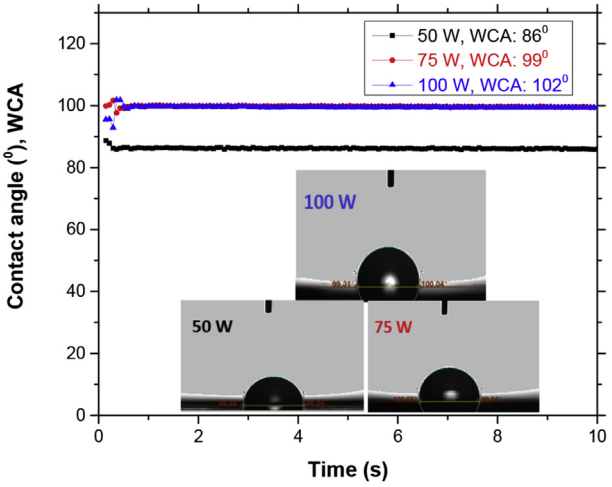

Fig. 7. For the VGNs, time-dependent variation of WCA is shown. It is understood that there is no change in the WCA values of VGNs over time. Furthermore, the images of the water droplet on the surface for each VGN are given in the inner-graph.

a nanoscale property.

4. Conclusion

VGNs were effectively produced on copper foils by using PECVD technique with various RF powers. Raman spectroscopy revealed that VGNs are 3D oriented and have an significant effect of RF power on the tightly packed structure of these vertically oriented (3D) nanostructures. It was understood that increased RF power significantly affected the presence of the 2D peak and the change in the intensity of this peak. From the SEM images, it was clearly demonstrated that the graphene was obtained vertically. A homogeneous structure was detected for the VGN obtained using 100 W RF power. This situation was not the same uniformity for other RF powers. The WCA analysis also showed that VGNs had a hydrophobic character and this angle was measured as 102° for 100 W RF power. These results were attributed to the presence of vertically oriented graphene as seen from the SEM images. The large surface areas of VGN indicate that they have the potential to be used in important areas such as solar cell, supercapacitor and li-ion batteries.

Acknowledgment

This study is dedicated to my father, Ilyas BAYRAM, who supported me throughout my academic life. I hope you sleep in peace forever. The authors are grateful to H. Fevzi Budak (SEM analysis), and A. Emre Kasapoglu (RAMAN analysis) from the East Anatolian high-tech research center (DAYTAM) for assisting in material characterization.

Appendix A. Supplementary data

Supplementary data to this article can be found online at https://doi.org/10.1016/j.ceramint.2019.04.034.

References

[1] K.S. Novoselov, et al., Electric field effect in atomically thin carbon films, Science 306 (5696) (2004) 666–669.
[2] E. Pop, V. Varshney, A.K. Roy, Thermal properties of graphene: fundamentals and applications, MRS Bull. 37 (12) (2012) 1273–1281.
[3] K.I. Bolotin, et al., Ultrahigh electron mobility in suspended graphene, Solid State Commun. 146 (9–10) (2008) 351–355.
[4] R.R. Nair, et al., Fine structure constant defines visual transparency of graphene, Science 320 (5881) (2008) 1308 1308.
[5] C. Lee, et al., Measurement of the elastic properties and intrinsic strength of monolayer graphene, Science 321 (5887) (2008) 385–388.
[6] Q. He, et al., Graphene-based electronic sensors, Chem. Sci. 3 (6) (2012) 1764–1772.
[7] W. Yuan, G. Shi, Graphene-based gas sensors, J. Mater. Chem. 1 (35) (2013) 10078–10091.
[8] L. Kavan, J.H. Yum, M. Graetzel, Application of graphene-based nanostructures in dye-sensitized solar cells, Phys. Status Solidi 250 (12) (2013) 2643–2648.
[9] X. Li, et al., Graphene-on-silicon Schottky junction solar cells, Adv. Mater. 22 (25) (2010) 2743–2748.
[10] Z.S. Wu, et al., Graphene-based in-plane micro-supercapacitors with high power and energy densities, Nat. Commun. 4 (2013) 2487.
[11] K.S. Novoselov, et al., A roadmap for graphene, Nature 490 (7419) (2012) 192.
[12] K.I. Bolotin, et al., Ultrahigh electron mobility in suspended graphene, Solid State Commun. 146 (9) (2008) 351–355.
[13] S. Amini, et al., Growth of large-area graphene films from metal-carbon melts, J. Appl. Phys. 108 (9) (2010) 094321.
[14] A. Tredicucci, M.S. Vitiello, Device concepts for graphene-based terahertz photonics, IEEE J. Sel. Top. Quantum Electron. 20 (1) (2014) 130–138.
[15] F. Bonaccorso, et al., Graphene photonics and optoelectronics, Nat. Photon. 4 (9) (2010) 611.
[16] C. Bautista-Flores, et al., Sulfur and few-layer graphene interaction under thermal treatments, Chem. Phys. Lett. 665 (2016) 121–126.
[17] G. Zhang, et al., Versatile polymer-free graphene transfer method and applications, ACS Appl. Mater. Interfaces 8 (12) (2016) 8008–8016.

[18] W. Gao, The chemistry of graphene oxide, Graphene Oxide, Springer, 2015, pp. 61–95.
[19] E. Yoo, et al., Large reversible Li storage of graphene nanosheet families for use in rechargeable lithium ion batteries, Nano Lett. 8 (8) (2008) 2277–2282.
[20] E. Yoo, et al., Enhanced electrocatalytic activity of Pt subnanoclusters on graphene nanosheet surface, Nano Lett. 9 (6) (2009) 2255–2259.
[21] A. Yu, et al., Ultrathin, transparent, and flexible graphene films for supercapacitor application, Appl. Phys. Lett. 96 (25) (2010) 253105.
[22] S. Vivekchand, et al., Graphene-based electrochemical supercapacitors, J. Chem. Sci. 120 (1) (2008) 9–13.
[23] Y. Sun, Q. Wu, G. Shi, Graphene based new energy materials, Energy Environ. Sci. 4 (4) (2011) 1113–1132.
[24] L.L. Zhang, R. Zhou, X. Zhao, Graphene-based materials as supercapacitor electrodes, J. Mater. Chem. 20 (29) (2010) 5983–5992.
[25] Z. Zhang, et al., Integrated polymer solar cell and electrochemical supercapacitor in a flexible and stable fiber format, Adv. Mater. 26 (3) (2014) 466–470.
[26] W. He, D. Geng, Z. Xu, Pattern evolution characterizes the mechanism and efficiency of CVD graphene growth, Carbon 141 (2019) 316–322.
[27] G.G. Politano, et al., Graphene oxide on magnetron sputtered silver thin films for SERS and metamaterial applications, Appl. Surf. Sci. 427 (2018) 927–933.
[28] E. Cazzanelli, et al., High-temperature evolution of linear carbon chains inside multiwalled nanotubes, Phys. Rev. B 75 (12) (2007) 121405.
[29] M. Castriota, et al., Spatial dependence of Raman frequencies in ordered and disordered monolayer graphene, Diam. Relat. Mater. 19 (5–6) (2010) 608–613.
[30] A. Cupolillo, et al., Second-order Raman scattering from linear carbon chains inside multiwalled carbon nanotubes, J. Raman Spectrosc.: Int. J. Orig. Work Aspect. Raman Spectrosc. Incl. Higher Order Process. Brillouin Rayleigh Scatt. 39 (2) (2008) 147–152.
[31] E. Cazzanelli, et al., Characterization of graphene grown on copper foil by chemical vapor deposition (CVD) at ambient pressure conditions, J. Raman Spectrosc. 49 (2018) 1006–1014.
[32] A. Policicchio, et al., Electronic, chemical and structural characterization of CNTs grown by SiC surface decomposition, Journal of Physics: Conference Series, IOP Publishing, 2008.
[33] M. Castriota, et al., Investigations on Raman bands from carbon linear chains in multiwalled carbon nanotubes, Diam. Relat. Mater. 17 (7–10) (2008) 1716–1723.
[34] M. Castriota, et al., Spatial dependence of Raman frequencies in ordered and disordered monolayer graphene, Diam. Relat. Mater. 19 (5) (2010) 608–613.
[35] G.G. Politano, et al., Physical investigation of electrophoretically deposited graphene oxide and reduced graphene oxide thin films, J. Appl. Phys. 120 (19) (2016) 195307.
[36] T.-o. Terasawa, K. Saiki, Growth of graphene on Cu by plasma enhanced chemical vapor deposition, Carbon 50 (3) (2012) 869–874.
[37] Z. Bo, et al., Plasma-enhanced chemical vapor deposition synthesis of vertically oriented graphene nanosheets, Nanoscale 5 (12) (2013) 5180–5204.
[38] H.G. Jain, et al., Carbon nanowalls deposited by inductively coupled plasma enhanced chemical vapor deposition using aluminum acetylacetonate as precursor, Carbon 49 (15) (2011) 4987–4995.
[39] Z. Ni, et al., Raman spectroscopic investigation of carbon nanowalls, J. Chem. Phys. 124 (20) (2006) 204703.
[40] N. Soin, et al., Microstructural and electrochemical properties of vertically aligned few layered graphene (FLG) nanoflakes and their application in methanol oxidation, Mater. Chem. Phys. 129 (3) (2011) 1051–1057.
[41] M.Y. Zhu, et al., Enhanced field emission of vertically oriented carbon nanosheets synthesized by C2H2/H2 plasma enhanced CVD, Carbon 49 (7) (2011) 2526–2531.
[42] J.N. Tiwari, et al., Direct synthesis of vertically interconnected 3-D graphitic nanosheets on hemispherical carbon particles by microwave plasma CVD, Plasmonics 6 (1) (2011) 67–73.
[43] J. Kim, et al., Low-temperature synthesis of large-area graphene-based transparent conductive films using surface wave plasma chemical vapor deposition, Appl. Phys. Lett. 98 (9) (2011) 091502.
[44] T. Yamada, et al., Low-temperature graphene synthesis using microwave plasma CVD, J. Phys. D Appl. Phys. 46 (6) (2013) 063001.
[45] A.C. Ferrari, D.M. Basko, Raman spectroscopy as a versatile tool for studying the properties of graphene, Nat. Nanotechnol. 8 (4) (2013) 235.
[46] R. Beams, L.G. Cançado, L. Novotny, Raman characterization of defects and dopants in graphene, J. Phys. Condens. Matter 27 (8) (2015) 083002.
[47] M. Dresselhaus, et al., Defect characterization in graphene and carbon nanotubes using Raman spectroscopy, Phil. Trans. Math. Phys. Eng. Sci. 368 (1932) (2010) 5355–5377.
[48] P. Tan, et al., Probing the phonon dispersion relations of graphite from the double-resonance process of Stokes and anti-Stokes Raman scatterings in multiwalled carbon nanotubes, Phys. Rev. B 66 (24) (2002) 245410.
[49] B. Li, D. Yu, S.-L. Zhang, Raman spectral study of silicon nanowires, Phys. Rev. B 59 (3) (1999) 1645.
[50] A. Reina, et al., Large area, few-layer graphene films on arbitrary substrates by chemical vapor deposition, Nano Lett. 9 (1) (2008) 30–35.
[51] A.P.A. Raju, et al., Wide-area strain sensors based upon graphene-polymer composite coatings probed by Raman spectroscopy, Adv. Funct. Mater. 24 (19) (2014) 2865–2874.
[52] X. Li, et al., Large-area synthesis of high-quality and uniform graphene films on copper foils, Science 324 (5932) (2009) 1312–1314.
[53] L. Liu, et al., High-yield chemical vapor deposition growth of high-quality large-area AB-stacked bilayer graphene, ACS Nano 6 (9) (2012) 8241–8249.
[54] L. Fang, et al., Growth of graphene on Cu foils by microwave plasma chemical vapor deposition: the effect of in-situ hydrogen plasma post-treatment, Appl. Surf. Sci. 383 (2016) 28–32.
[55] S. Kurita, et al., Raman spectra of carbon nanowalls grown by plasma-enhanced chemical vapor deposition, J. Appl. Phys. 97 (10) (2005) 104320.
[56] L. Cançado, et al., General equation for the determination of the crystallite size L a of nanographite by Raman spectroscopy, Appl. Phys. Lett. 88 (16) (2006) 163106.
[57] A.C. Ferrari, Raman spectroscopy of graphene and graphite: disorder, electron–phonon coupling, doping and nonadiabatic effects, Solid State Commun. 143 (1–2) (2007) 47–57.
[58] X. Guo, et al., Vertical graphene nanosheets synthesized by thermal chemical vapor deposition and the field emission properties, J. Phys. D Appl. Phys. 49 (38) (2016) 385301.
[59] Q. Yu, et al., Graphene segregated on Ni surfaces and transferred to insulators, Appl. Phys. Lett. 93 (11) (2008) 113103.
[60] Y. Sui, et al., Growth promotion of vertical graphene on SiO2/Si by Ar plasma process in plasma-enhanced chemical vapor deposition, RSC Adv. 8 (34) (2018) 18757–18761.
[61] J. Sun, et al., Direct low-temperature synthesis of graphene on various glasses by plasma-enhanced chemical vapor deposition for versatile, cost-effective electrodes, Nano Res. 8 (11) (2015) 3496–3504.
[62] N. Zhang, et al., Direct synthesis of vertical graphene nanowalls on glass substrate for thermal management, Mater. Res. Express 5 (6) (2018) 065606.
[63] M. Othman, et al., Low-temperature plasma-enhanced chemical vapour deposition of transfer-free graphene thin films, Mater. Lett. 158 (2015) 436–438.
[64] H. Ci, et al., 6-inch uniform vertically-oriented graphene on soda-lime glass for photothermal applications, Nano Res. 11 (6) (2018) 3106–3115.
[65] S. Ghosh, et al., Process-specific mechanisms of vertically oriented graphene growth in plasmas, Beilstein J. Nanotechnol. 8 (2017) 1658–1670.
[66] M.V. Jacob, et al., Catalyst-free plasma enhanced growth of graphene from sustainable sources, Nano Lett. 15 (9) (2015) 5702–5708.
[67] Pekdemir Sami, M. Serdar Onses, Mehmet Hancer, Low temperature growth of graphene using inductively-coupled plasma chemical vapor deposition, Surf. Coating. Technol 309 (2017) 814–819.